Colloids and Surfaces B: Biointerfaces 202 (2021) 111686

Contents lists available at ScienceDirect

Colloids and Surfaces B: Biointerfaces

journal homepage: www.elsevier.com/locate/colsurfb

An amplified fluorescent biosensor for Ag^+ detection through the hybridization chain reactions

Hengxuan Li [a,1], Minghui Chen [a,b,1], Ran Luo [a], Weipan Peng [a], Xiaoqun Gong [a,*], Jin Chang [a,*]

[a] School of Life Sciences, Tianjin University and Tianjin Engineering Center of Micro-Nano Biomaterials and Detection-Treatment Technology (Tianjin), Tianjin 300072, China

[b] School of Medical Imaging, Xuzhou Medical University, Xuzhou, China

ARTICLE INFO

Keywords:
Ag^+
Hybridization chain reaction
Fluorescence signal
Water quality testing

ABSTRACT

Ag is widely distributed in nature and it is used in almost all areas of human life. However, due to the widespread use of Ag materials, Ag^+ pollution seriously threatens the human health and environment. The traditional detection methods for Ag^+ suffer from disadvantages including high operational cost, complicated operating unit and instrument, and high requirements for professionals. Thus, in this study, a new type of Ag^+ detection biosensor based on the hybridization signal amplification was designed to overcome these problems. Combining cytosine-Ag^+-cytosine mismatch structure with the hybridization chain reaction, this biosensor converted the conventional detection signal into the nucleic acid amplification signal, which realized efficient, rapid, sensitive, and specific detection of Ag^+. The limit-of-detection of this sensor reached 0.69 pM, which is much less than the maximum concentration (0.1 mg L^{-1}, 927 nM) suggested for drinking water by the World Health Organization, and the maximum concentration (0.05 mg L^{-1}, 464 nM) suggested by the United States Environmental Protection Agency. This method provides a promising new platform for detecting Ag^+ concentrations at ultralow levels.

1. Introduction

As one of the most common precious metal elements in the world, silver (Ag) and its ionic form (Ag^+) are widely used in industry and daily life [1]. However, Ag^+ has been recognized as an ion with the highest toxic level, thus attracting widespread research attention for remediation of the potential risks caused by its extensive use [2]. Ag^+ is a type of pollutants capable of causing extensive damages to the nerves and internal organs [3]. If a large amount of Ag^+ gets released into the environment, it can accumulate in the food chain [4–8]. When Ag^+ enters the human body, it can interact with several groups of metabolites, leading to the inactivation of sulfhydryl enzymes [9,10]. According to the U.S. Environmental Protection Agency (EPA), when the concentration of Ag^+ is above 1.6 nM, there is possibility of poisoning of fish and microorganisms in the water bodies. Moreover, the permitted concentration of Ag^+ for safe drinking water should not exceed 930 nM [11–14]. Therefore, there is an urgent requirement to determine trace Ag^+ for environmental monitoring, biological conservation, and alleviation of risks to human health.

Traditional methods of Ag^+ detection include inductively coupled plasma-mass spectrometry (ICP-MS), inductively coupled plasma-atomic emission spectroscopy (ICP-AES), atomic absorption spectrometry, and fluorescence spectroscopy [15–25]. However, these methods are time-consuming, expensive, and require large instruments and skilled operations [26]. These disadvantages limit the application of traditional detection methods in areas without abundant resources [27]. Moreover, fluorescence colorimetric approach is regarded as a simple and useful detection technique, which can be used for quantitative characterization of the concentration of target objects based on inexpensive spectrometers and simple operations [28–30]. However, compared to the above-mentioned traditional detection methods, the bottleneck for the colorimetric methods showed that the detection limit was confined to the nM level, which is not sensitive enough [31–33]. Therefore, development of a simple, convenient, efficient, highly sensitive, and selective Ag^+ sensing method is highly desirable.

Hybridization chain reaction (HCR) is an isothermal enzyme-free nucleic acid amplification technology first discovered and reported by Pierce and Dirks. HCR is widely applied for sensitive and specific detection of substances, such as proteins and small molecules [34–36]. It is driven by the free energy of base pair formation without the enzymatic

* Corresponding authors.
E-mail addresses: gongxiaoqun@tju.edu.cn (X. Gong), jinchang@tju.edu.cn (J. Chang).
[1] Authors who contributed equally to this work.

https://doi.org/10.1016/j.colsurfb.2021.111686
Received 26 January 2021; Received in revised form 4 March 2021; Accepted 7 March 2021
Available online 8 March 2021

catalysis; however, the occurrence of three cycles of deformation, annealing, and extension of polymerase chain reaction (PCR) [37–39] is not required. As a result of initiation, HCR can effectively reduce the false positive signal and the background disturbance [40]. Moreover, each initiator triggers HCR to form long-chain dsDNA, which links a number of oligonucleotides to amplify the sensor signal [34,41,42]. Further, the HCR can be carried out under mild conditions and monitored easily. Therefore, the HCR may be of great assistance to increase the sensitivity of Ag^+ detection.

Herein, a simple, efficient, and sensitive method was developed for analysis and detection of Ag^+ by introducing nucleic acid hybridization signals on the platform of silica (SiO_2) microspheres. As a strong and specific binding interaction of cytosine-Ag^+-cytosine (C-Ag^+-C) mismatch structures, DNA probes designed with several cytosine bases were used to identify Ag^+, which could significantly improve the specificity of the sensor. Moreover, with the high enzyme-free isothermal nucleic acid amplification of HCR, this sensor could achieve a high sensitivity and large analytical range of Ag^+ by detecting the fluorescence signal of Cy5 labeled on the probes. Finally, the specificity of the sensor and the detection capability in the actual sample were also examined, and the results were compared with those of standard Ag^+ detection methods. The designed sensor could realize cost effectiveness, high specificity, and sensitivity for Ag^+ detection.

2. Material and methods

2.1. Materials

All HPLC-purified oligonucleotides sequences were provided by Sangon Biotech Co., Ltd. (Shanghai, China). 1-(3-Dimethylaminopropyl)-3-ethylcarbodiimide hydrochloride (EDC, cat. no. 39311) and silver nitrate were obtained from Aladdin (Shanghai, China). Diethyl pyrocarbonate (DEPC)-treated water used for preparing and diluting the oligonucleotides solutions was provided by Sangon Biotech Co., Ltd. (Shanghai, China). Deionized water (≥18 MΩ) was used in the preparation of all other chemicals which were of analytical grade and used as received. All buffers and mixtures used in the experiment were prepared with sterile water. Amine-functionalized SiO_2 nanoparticles (SiO_2-NH_2) were purchased from NewMater™ Nanotechnology Co., Ltd. (China). Affimag SLC magnetic microspheres were purchased from BaseLine ChromTech Research Center (TianJin, China). Oligonucleotides sequences used in this study are listed in Table S1. Phosphate buffered saline (PBS, DNAase free, RNAase free, 0.01 M, pH = 7.2–7.5), phosphate buffered solution, and saline sodium citrate (SSC) buffer were purchased from SenBeiJia Biological Technology Co., Ltd. (Nanjing, China). Agarose, SuperGel Red nucleic acid dye; and tris base, acetic acid, and EDTA (TAE) buffer were all obtained from Biosharp (Hefei, China). The bioluminescent 96-well white microplate was purchased from Thermo Fisher Scientific (Pittsburgh, USA). The electrophoresis equipment was obtained from Bio-Rad (USA). The bioluminescent signal receptor used in this study was Azure®C600 (USA). Other reagents used in this experiment were of analytical grade and used as received without any further purification.

2.2. Electrophoresis experiment for feasibility verification

Electrophoresis was performed to verify the feasibility of the experiment. Different primers in the reaction were analyzed by using 3 % agarose gel electrophoresis in 1 × TBE buffer at room temperature. For each lane, the final concentration of each single strand was 1 u M, and the total volume was 20 μL. P1, P2, the mixture of P1, P2 and Ag^+, H1, H2 were loaded in lanes 1–5, respectively. Lanes 6 and 7 were parallel-controlled as two experimental groups. In the lane 6, Ag^+ (10 μL, 10^{-7} M) was added and in the lane 7, the equal amount of SSC buffer was added instead of Ag^+. They were allowed to complete the entire conventional reaction, centrifuged to remove the supernatant, and the precipitate was washed repeatedly to avoid the interference of the non-specific adsorption of Cy5 fluorescence in the control group. Then the reaction system was heated to 95 °C, the nucleic acid probe was separated from the SiO_2 microspheres, samples were centrifuged again, and the supernatant was taken for the agarose gel (3 %) electrophoresis. The electrophoresis was carried out at a constant voltage of 110 V for 70 min. Then the agarose gel (3 %) was captured by fluorescence channels.

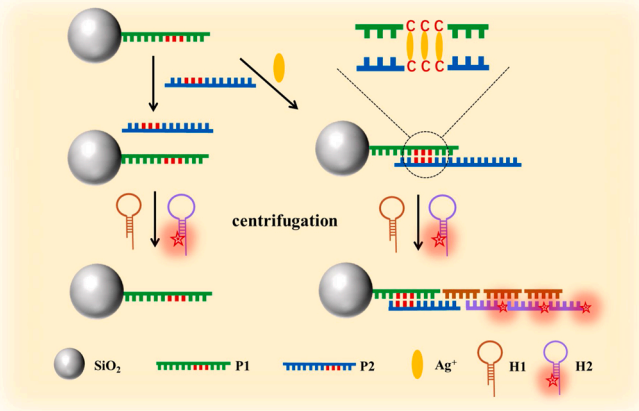

Scheme 1. The principle of the sensor for ultra-sensitive Ag^+ detection.

2.3. Preparation of DNA-SiO_2 conjugates

The designed DNA probes 1 and 2 (P1 and P2) were diluted to 100 or 10 μM as required. EDC (1 mg) was weighed and placed in a 1.5 mL round bottomed centrifuge tube. Then, the aminated modified SiO_2 microspheres (500 μL, 5 mg mL^{-1}) and P1 (50 μL, 10 μM) were added and mixed thoroughly. The tube was wrapped with tin foil as a dark-proof treatment, and incubated for 10 h. After the reaction was completed, the reaction system was centrifuged at 10,000 rpm for 10 min, and resuspended with ddH_2O (200 μL) after the removal of the supernatant. Finally, SiO_2-DNA probe 1 conjugates (SiO_2-P1) were obtained and stored at 4 °C.

2.4. Quantification detection of Ag^+

SiO_2-P1 (10 μL) ligated in step 2.3 and P2 (0.7 μL, 10 μM) were added to sodium citrate-citrate buffer (25 μL). Then H1 (1.5 μL, 1 μM) and 1 Cy5-H2 (1.5 μL, 1 μM) were added to the reaction system. Finally, the appropriate concentration of target Ag^+ was added and mixed thoroughly, and the reaction system was incubated at 37 °C for 60 min. After the completion of the reaction, the supernatant was removed by centrifugation at 11,000 rpm for 10 min using a centrifuge, and the precipitate was resuspended in water (50 μL). Subsquently, the Cy5 fluorescence signal intensity was measured using Azure C600 for several min.

2.5. Specificity investigation of the sensor

The specificity of this sensor was controlled by the nucleotide sequence of P1. The specificity investigation experiments were carried out by incubating Ag^+ (10 μL, 1 × 10^{-7} M) and different kinds of metal ion (negative control, Mg^{2+}, Na^+, K^+, Ca^{2+}, Cd^{2+}, Cu^{2+}, Fe^{3+}, Zn^{2+}, Mn^{2+}, Ni^{2+}, mixed group) at the same concentration of 1 × 10^{-7} M. Then, the same procedures were carried out by step 2.4.

2.6. Ag^+ detection in real water samples

In order to evaluate the practicality of sensors for real water samples, five different actual water samples were detected by ICP-MS and ICP-

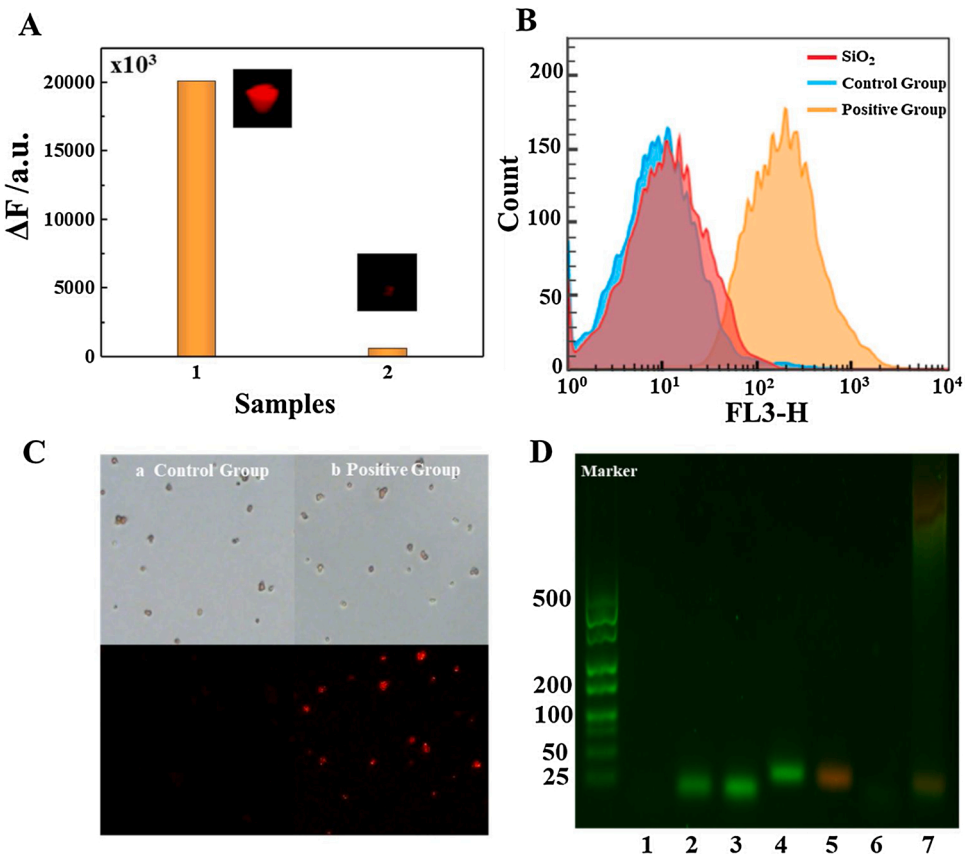

Fig. 1. (A) Visualization photograph and fluorescence of preliminary feasibility study of quantitative determination of Ag^+: (1): 1×10^{-7} M Ag^+, (2): 0 M Ag^+. (B) The flow cytometry intensity result of SiO_2 microspheres, control group (without Ag^+) and positive group (with Ag^+). (C) The fluorescent microscopy images of (a) control group and (b) positive group in bright field and dark field, respectively. (D) The illustration of reaction mixture for the agarose gel (3 %) electrophoresis carried out for the feasibility study of the sensors, were captured by RGB channels. (1) P1, (2) P2, (3) P1, P2, and Ag^+, (4) H1, (5) H2 were injected during the agarose gel (3 %) electrophoresis. (6)–(7): In the absence (6) and presence (7) of Ag^+, P1, P2, H1, and H2, the entire reaction was completed, the contents were heated to 95 °C for 7 min, and the supernatant was directly injected for the agarose gel (3 %) electrophoresis after high speed centrifugation.

AES, respectively, and compared with the sensor. In addition, a series of Ag^+ samples were added to pure water by a standard addition method with the same concentration, the Ag^+ concentration of each sample was measured by the sensor and compared with the actual concentration. The lake water samples were collected from the Tianjin University.

3. Results and discussion

3.1. The principle of HCR fluorescent sensor

The working principle of the sensor for Ag^+ detection is illustrated in Scheme 1. The C-Ag^+-C structure was introduced to realize the specific detection of Ag^+, and the HCR efficient amplification was employed to obviously improve the detection sensitivity. SiO_2 microspheres as the signal carriers were decorated with P1. H2 was labeled with fluorescent dye Cy5 (Ex:650 nm, Em:670 nm). In the presence of Ag^+, P1 and P2 combined to form C-Ag^+-C structure. The SiO_2 microspheres with C-Ag^+-C structure were separated by centrifugation to initiate HCR. The HCR mechanism employed two hairpin species (H1 and H2). Furthermore, introduction of an initiator strand (P2) triggered a chain reaction of alternating kinetic escapes by continuously opening the H1 and H2 stem-loop structure. Amplification of the initiator recognition event continued until the supply of H1 or H2 was exhausted [34]. The fluorescent signal of Cy5 could be detected on the surface of SiO_2 microspheres, which was proportional to the concentration of Ag^+. In this study, Azure C600 was introduced to quantify the fluorescent intensity.

3.2. Research on the feasibility of the HCR fluorescent sensor

In order to verify the feasibility of the HCR fluorescent sensor, experiments were performed on two Ag^+ samples with different concentrations, and the corresponding results are shown in Fig. 1. The experiment in presence of Ag^+ (10^{-7} M) and absence of Ag^+ (0 M) were performed in the Fig. 1A. As we can see, the sample with Ag^+ had stronger fluorescence signal compared with the sample without Ag^+. The ultraviolet (UV) absorbance values of SiO_2 microspheres, SiO_2-P1-P2-HCR conjugates, and P1 were measured by UV–vis spectrophotometer, respectively. Fig. S1 illustrates the absence of the absorbance between 240 and 290 nm on SiO_2 microspheres. Owing to the HCR efficient amplification, hundreds of double-stranded nucleotides (nt) were formed on the SiO_2 microspheres in the presence of Ag^+ [34]. Therefore, the absorbance of SiO_2-P1-P2-HCR conjugates between 240 and 290 nm increased significantly with a significant absorption at 260 nm, indicating that DNA probes and the HCR system were attached to the surface of SiO_2 microspheres successfully.

Furthermore, the flow cytometry and fluorescent microscopy were employed to verify that the HCR system could be generated on SiO_2 microspheres. In the presence of Ag^+, the HCR system was connected to the surface of SiO_2 microspheres by C-Ag^+-C structure, and the Cy5 fluorescence signal was detected using the flow cytometer and microscope (Fig. 1B and C). In control group, there were ignorable Cy5 fluorescence signal detected in the absence of Ag^+ (Fig. 1C). It indicated that only in the presence of Ag^+, the Cy5 fluorescence signal could be generated on SiO_2 microspheres correspondingly. The scatter diagram results of each group are shown in Fig. S2, demonstrating that Ag^+ was the vital initiator for connecting HCR system with SiO_2 microspheres.

The reaction mixture for the agarose gel (3 %) electrophoresis was used for the feasibility study of the sensors. Fig. 1D demonstrates that there was no band in the first lane, because the length of P1 was only 10 nt and the marker showed at least 25 nt. The brightness of band in lane 3 was higher than that in lane 2, indicating that P1 connected P2 together in the presence of Ag^+. Furthermore, after incubation, centrifugation, and separation, nucleic acid strands with Cy5 were detected in lane 7, the length of strands ranged from tens to hundreds of nt, and there was no fluorescence signal detected in lane 6. It was thus revealed that the HCR system was attached to the SiO_2 microspheres by C-Ag^+-C

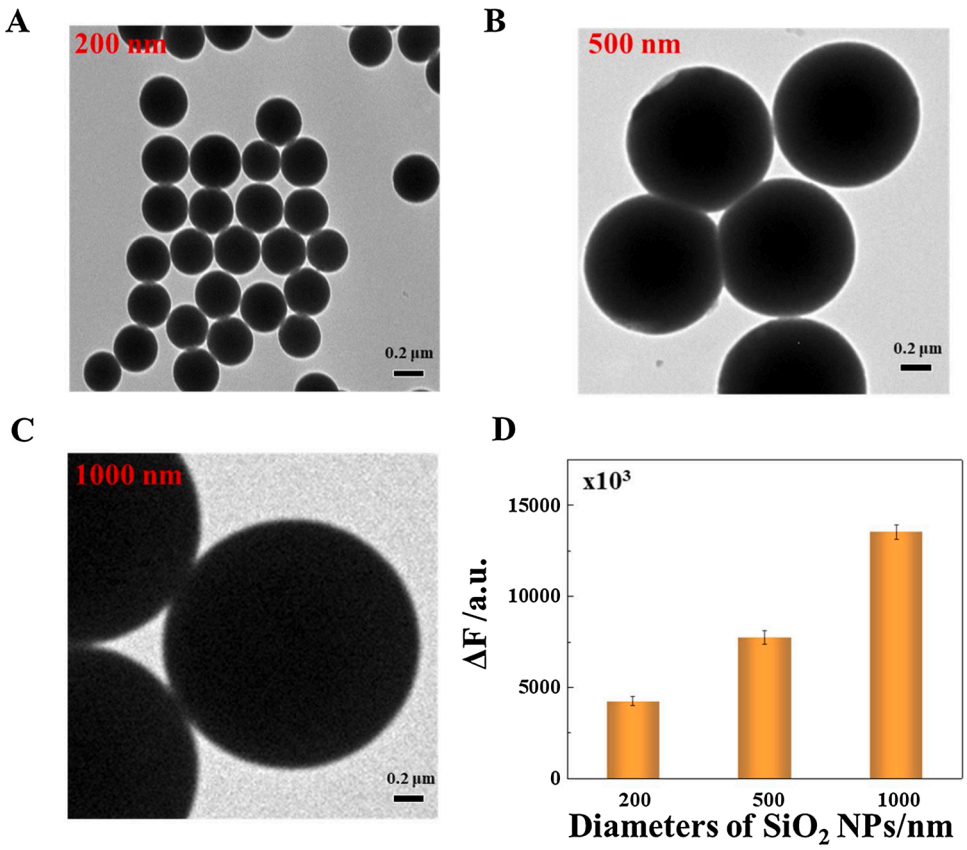

Fig. 2. (A)–(C) TEM images of SiO_2 microspheres with different diameters (200, 500, and 1000 nm); (D) Analysis of HCR fluorescent sensor detection with different sizes of SiO_2 microspheres. n = 3 independent experiments. Error bars represent the standard deviation of triplicates.

mismatch structure.

3.3. Evaluation and Optimization of experimental conditions

Furthermore, the size of SiO_2 microspheres, the sequences of P1 and P2, the type of carrier and buffer solution, the incubation temperature, and the time were optimized. SiO_2 microspheres were used to build a signal amplification carrier. More DNA probes could be loaded on the surface of SiO_2 microspheres because of the spherical structure, thus it was necessary to explore the optimal diameters of SiO_2 microspheres for higher sensitivity. Different sizes (200, 500, and 1000 nm) of SiO_2 microspheres were discussed. Fig. 2 exhibits that the value of ΔF (ΔF = F – F0, F0 and F stand for the fluorescence obtained in the absence and presence of Ag^+, respectively) enhanced with the increase of the diameter. Thus, SiO_2 microspheres with diameter of 1000 nm were used in our sensor.

The incubation temperature and time were studied by employing the variable control method. To achieve the most suitable reaction temperature, a series of different temperatures was optimized, and the results are shown in Fig. 3. The stability of the reaction in the range of 4–37 °C increased gradually, and the fluorescence intensity was the highest at 37 °C (Fig. 3A). The fluorescence intensity decreased at 45 °C due to the disassembly of the C-Ag^+-C structure at higher temperature. Therefore, 37 °C was selected as the optimal temperature for subsequent experiments. Then, a series of different time was optimized. The results indicated that fluorescence intensity enhanced with the increase of reaction time within an appropriate range, which is shown in Fig. 3B. When the reaction time reached 60 min, the fluorescence intensity could not change sharply. Considering the low-cost principle, 60 min was selected as the optimal time. Moreover, Figs. S3–S5 demonstrate that other experimental conditions were also determined. The sequences of P1 and P2 were defined, the SiO_2 microspheres were selected as the carrier, and the sodium citrate buffer was selected as the buffer solution.

In order to increase the detection sensitivity, the amounts of SiO_2-P1, P2, H1, and H2 were also investigated. The reaction was carried using SiO_2 microspheres, and the amount of SiO_2-P1 played an important role in the detection of Ag^+. Fig. 3C exhibits that the ΔF value enhances with the increase of the amount of SiO_2-P1 until 15 μL. Other parameters for detecting Ag^+ were also investigated by employing the experimental plan presented in Fig. 3C. The concentration of P1, H1, and H2 was closely related to the amplification of the detection signal. Fig. 3D–F exhibit that P2 (350 nM), H1 (150 nM), and H2 (150 nM) were selected to obtain the best sensitivity.

3.4. Detection performance of the HCR fluorescent sensor

The detection performance of the sensor mainly included the detection sensitivity and specificity. Under the optimal conditions, Ag^+ standards with different concentrations (10^{-12}–10^{-8} M) were monitored (Fig. 4). Fig. 4A exhibits that a linear relationship between the ΔF and the logarithm of Ag^+ level correlates to the data points ($\Delta F = 19{,}045.99 + 1318.95 \lg C$, $R^2 = 0.9948$). The limit-of-detection (LOD) of Ag^+ was 0.69 pM (LOD = 3S/N, where S is standard deviation value of blank samples, and N is the slope of the standard curve for low concentration), which fell far below the threshold value for drinking water, specified by EPA.

Anti-interference ability is an important standard to measure the excellence of a sensor. The specific binding of Ag^+ to C–C base pairs was used for our sensor, which indicates that it should not respond to other common metal ions. As expected, compared to Ag^+ (10^{-7} M), none of the following metal ions including Mg^{2+}, Na^+, K^+, Ca^{2+}, Cd^{2+}, Cu^{2+}, Fe^{3+}, Zn^{2+}, Mn^{2+}, and Ni^{2+} at a concentration of 10^{-7} M, respectively, showed a significant response to the sensor. Moreover, the sample containing mixed Ag^+ and Mg^{2+}, Na^+, K^+, Ca^{2+}, Cd^{2+} Cu^{2+}, Fe^{3+}, Zn^{2+}, Mn^{2+}, or

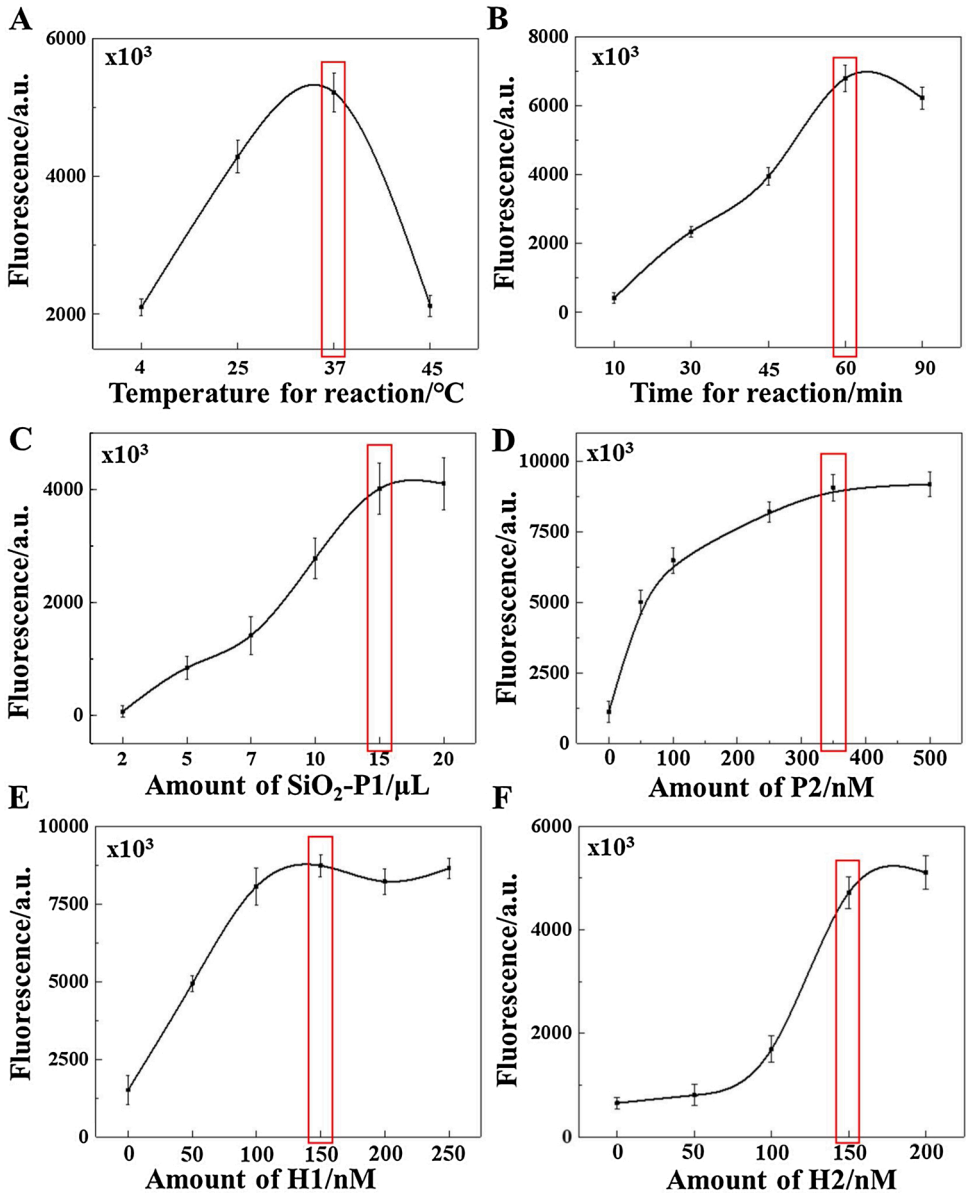

Fig. 3. Optimization experiments of (A) reaction temperature; (B) reaction time; (C) amount of SiO_2-P1; (D) concentration of P2; (E) concentration of H1; and (F) concentration of H1. n = 3 independent experiments. Error bars represent the standard deviation of triplicates.

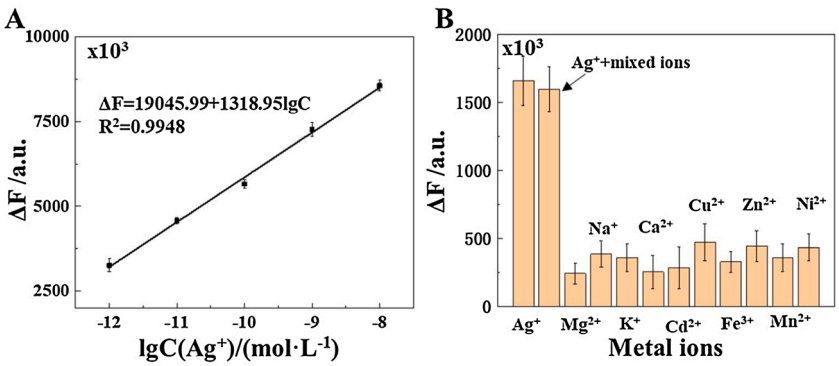

Fig. 4. (A) The linear response between ΔA and the logarithm of Ag^+ concentration ranging from 10^{-12} to 10^{-8} M. (B) Specificity assay for the sensor to several common metal ions (Ag^+, Mg^{2+}, Na^+, K^+, Ca^{2+}, Cd^{2+}, Cu^{2+}, Fe^{3+}, Zn^{2+}, Mn^{2+}, Ni^{2+}, and mixed ions). n = 3 independent experiments. Error bars represent the standard deviation of triplicates.

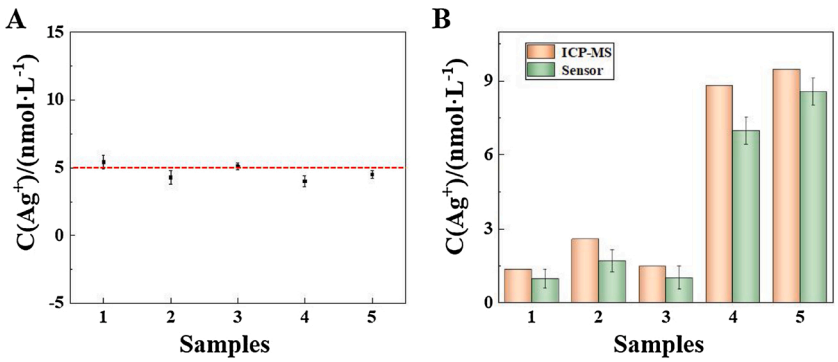

Fig. 5. (A) Use of standard addition method for the determination of Ag^+. Ag^+ was added as standard into ddH_2O with a concentration of 5×10^{-9} M. Five samples were detected in parallel by the sensor. (B) Detection of Ag^+ from several different real water samples by ICP-MS and the sensor: (1) Drinking water, (2) Tap water, and (3)–(5) Water from three different lakes. n = 3 independent experiments. Error bars represent the standard deviation of triplicates.

Ni^{2+} at a concentration of 10^{-7} M showed the fluorescence similar to the sample containing only Ag^+. Obviously, these results shown in Fig. 4B indicated that the interference of the metal ions (frequently appearing in the environment) to the sensor was negligible; thus, the sensor showed an excellent selectivity.

Furthermore, the stability and reproducibility of the sensor for detection was assessed via standard addition method (the same certain amount of Ag^+ standard was added into five different diluted salivary samples with the final concentration of 5×10^{-9} M). The calibration curve of fluorescence value versus concentration of Ag^+ obtained using our sensor is shown in Fig. S6, and a good agreement between spiked and detected concentration was obtained for quantification of Ag^+ (Fig. 5). Table S2 summarizes that the specific percent recovery was calculated to be in the range from 80.2 to 108.4 %. Moreover, the statistical analysis was carried out by the Welch's unpaired *t*-test for this recovery experiment (Table S3). The P-value for the detection of Ag^+ was 0.238973 ($P > 0.05$), and these results indicated that the detection results of Ag^+ with our sensor were not statistically different from the theoretical values (red dotted lines in Fig. 5A) and showed an excellent stability and reproducibility for Ag^+ detection.

3.5. Application of the HCR fluorescent sensor for detecting Ag^+ in real samples

Encouraged by the high sensitivity and selectivity of the sensor toward Ag^+, we further extended the investigation of determination ability in real water samples. The real water samples were collected from drinking water, tap water, and three different lakes in Tianjin University. The water samples were filtered through 0.22 μM nitrocellulose membranes to dispose of physical impurities prior to measurement. Noteworthy, no signal in the actual samples was detected by ICP-AES (Agilent 7500ce); however, the concentration of Ag^+ in the real water samples was detected by our sensor and ICP-MS (Agilent 7700X). Fig. 5B exhibits that the concentrations of Ag^+ in these five actual samples were separately obtained. Considering the influence of numerous minerals and organics existing in actual samples, there was no significant difference between our sensor and ICP-MS. Moreover, the results showed that the sensitivity of our sensor was superior to that of some traditional Ag^+ detection methods such as ICP-AES. Taken together, these results suggested that the Ag^+ biosensor proposed herein shows potential applicability in real samples.

4. Conclusions

Herein, an ultra-sensitive Ag^+ detection method was demonstrated that achieved picomolar level detection via HCR amplification strategy. The high selectivity and sensitivity of this method were based on C-Ag^+-C specific structure and HCR amplification strategy, respectively. The LOD of our sensor reached 0.69 pM ultimately, which is far below the threshold of the Ag standard in drinking water (930 nM) permitted by the EPA. Moreover, it was further proved that the sensor was effective for detection of actual samples by detecting Ag^+ in lake water and tap water samples, and the results were further compared with those of the ICP-MS. The Ag^+ biosensor shows application prospect in environmental monitoring with ultralow levels.

Data availability

All data are available without restriction. All relevant data are within the paper.

CRediT authorship contribution statement

Hengxuan Li: Conceptualization, Methodology, Formal analysis, Writing - original draft. **Minghui Chen:** Conceptualization, Methodology, Formal analysis, Writing - original draft. **Ran Luo:** Investigation, Funding acquisition. **Weipan Peng:** Investigation, Funding acquisition. **Xiaoqun Gong:** Visualization, Writing - review & editing, Funding acquisition, Project administration, Funding acquisition, Validation. **Jin Chang:** Visualization, Writing - review & editing, Funding acquisition, Project administration, Funding acquisition, Validation.

Declaration of Competing Interest

The authors report no declarations of interest.

Acknowledgements

The authors greatly acknowledge the financial support from the National Natural Science Foundation of China (31600800), Tianjin Natural Science Foundation (15JCQNJC03100), the key technologies R&D program of Tianjin (16ZXMJSY00010), and the Seed Foundation of Tianjin University (2017XYF-0013).

Appendix A. Supplementary data

Supplementary material related to this article can be found, in the online version, at doi:https://doi.org/10.1016/j.colsurfb.2021.111686.

References

[1] F. Yu, M. Lan, Z. Xi, Z. Jiang-Lin, R. Carl, N. Xin-Long, Y. Takehiko, An NBD-armed thiacalix[4]arene-derived colorimetric and fluorometric chemosensor for Ag^+: a metal-ligand receptor of anions, Dalton Trans. 42 (2013) 3552–3560.
[2] H. Xi, M. Cui, L. Wei, Z. Chen, Colorimetric detection of Ag^+ based on C-Ag^+-C binding as a bridge between gold nanoparticles, Sens. Actuators B 250 (2017) 641–646.

[3] R.B. Naik, S.B. Jagtap, R.S. Naik, N.G. Malvankar, D. Ratna, Effect of non-ionic surfactants on thermomechanical properties of epoxy/multiwall carbon nanotubes composites, Prog. Org. Coat. 77 (2014) 1883–1889.
[4] R.B. Naddy, J.W. Gorsuch, A.B. Rehner, G.R. McNerney, R.A. Bell, J.R. Kramer, Chronic toxicity of silver nitrate to Ceriodaphnia dubia and Daphnia magna, and potential mitigating factors, Aquat. Toxicol. 84 (2007) I–X.
[5] K. Vijayavel, Water chemistry influences the toxicity of silver to the green-lipped mussel Perna viridis, Environ. Monit. Assess. 167 (2010) 289–295.
[6] Y. Zhang, H. Obata, T. Gamo, Silver in Tokyo Bay estuarine waters and Japanese rivers, J. Oceanogr. 64 (2008) 259–265.
[7] N. Saha, M.Z.I. Mollah, M.F. Alam, M.S. Rahman, Seasonal investigation of heavy metals in marine fishes captured from the Bay of Bengal and the implications for human health risk assessment, Food Control 70 (2016) 110–118.
[8] M.S. Achary, K.K. Satpathy, S. Panigrahi, A.K. Mohanty, R.K. Padhi, S. Biswas, R. K. Prabhu, S. Vijayalakshmi, R.C. Panigrahy, Concentration of heavy metals in the food chain components of the nearshore coastal waters of Kalpakkam, southeast coast of India, Food Control 72 (2017) 232–243.
[9] R. Mikelova, J. Baloun, J. Petrlova, V. Adam, L. Havel, H. Petrek, A. Horna, R. Kizek, Electrochemical determination of Ag-ions in environment waters and their action on plant embryos, Bioelectrochemistry 70 (2007) 508–518.
[10] L.C. Murfin, C.M. Lopez-Alled, A.C. Sedgwick, J. Wenk, T.D. James, S.E. Lewis, A simple, azulene-based colorimetric probe for the detection of nitrite in water, Front. Chem. Sci. Eng. 14 (2020) 90–96.
[11] Y. Hong, Z. Zhou, F. Li, Y. Tao, C. Huang, New Hg^{2+} and Ag^{+} selective colorimetric sensor based on thiourea subunits, Inorg. Chem. Commun. 10 (2007) 1136–1139.
[12] Q. Li, Y. Kim, J. Namm, A. Kulkarni, G.R. Rosania, Y.H. Ahn, Y.T. Chang, RNA-selective, live cell imaging probes for studying nuclear structure and function, Chem. Biol. 13 (2006) 615–623.
[13] J.W. Ding, W. Qin, Y. Zhang, X.W. Wang, Potentiometric aptasensing based on target-induced conformational switch of a DNA probe using a polymeric membrane silver ion-selective electrode, Biosens. Bioelectron. 45 (2013) 148–151.
[14] D.P. Kafetzopoulos, E.L. Psomas, P.D. Kafetzopoulos, Measuring the effectiveness of the HACCP food safety management system, Food Control 33 (2013) 505–513.
[15] R. Gao, G. Xu, L. Zheng, Y. Xie, M. Tao, W. Zhang, A highly selective and sensitive reusable colorimetric sensor for Ag^{+} based on thiadiazole-functionalized polyacrylonitrile fiber, J. Mater. Chem. 4 (2016) 5996–6006.
[16] M.J. Ping, W.S. Qing, Z.C. Wei, W.H. Ying, D.Y. Bin, Cu(II)4L4 coordination-driven molecular container: a reusable visual colorimetric sensor for Ag(I) ions, Chem. Commun. 50 (2014) 4721–4724.
[17] A. Kumar, V. Kumar, U. Diwan, K.K. Upadhyay, Highly sensitive and selective naked-eye detection of Cu^{2+} in aqueous medium by a ninhydrin–quinoxaline derivative, Sens. Actuators B 176 (2013) 420–427.
[18] T. Liu, G. Li, N. Zhang, Y. Chen, An inorganic–organic hybrid optical sensor for heavy metal ion detection based on immobilizing 4-(2-pyridylazo)-resorcinol on functionalized HMS, J. Hazard. Mater. 201 (2012) 155–161.
[19] Y. Zhang, C.F. Zhu, L. Zhang, C.L. Tan, J. Yang, B. Chen, L.H. Wang, H. Zhang, DNA-templated silver nanoclusters for multiplexed fluorescent DNA detection, Small 11 (2015) 1385–1389.
[20] W. Guo, S.H. Hu, J.Y. Zhang, H.F. Zhang, Elimination of oxide interferences and determination of ultra-trace silver in soils by ICP-MS with ion-molecule reactions, Sci. Total Environ. 409 (2011) 2981–2986.
[21] W. Huang, Y. Liang, Y.Q. Deng, Y.H. Cai, Y. He, Prussian Blue nanoparticles as optical probes for visual and spectrophotometric determination of silver ions, Microchim. Acta 184 (2017) 2959–2964.
[22] Z.B. Guo, Y.F. Zheng, H. Xu, B.D. Zheng, W.W. Qiu, G.D. Liu, Lateral flow test for visual detection of silver(I) based on cytosine-Ag(I)-cytosine interaction in C-rich oligonucleotides, Microchim. Acta 184 (2017) 4243–4250.
[23] H.Z. Jiao, L. Zhang, Z.H. Liang, G.H. Peng, H.W. Lin, Size-controlled sensitivity and selectivity for the fluorometric detection of Ag^{+} by homocysteine capped CdTe quantum dots, Microchim. Acta 181 (2014) 1393–1399.
[24] J.K. Adu, D. Fafanyo, E. Orman, I. Ayensu, C.D.K. Amengor, S. Kwofie, Assessing metal contaminants in milled maize products available on the Ghanaian market with Atomic Absorption Spectrometry and Instrumental Neutron Activation Analyser techniques, Food Control 109 (2020).
[25] M.H. Chen, H.X. Li, D.M. Zhou, W.P. Peng, G.W. Lian, W.C. Gao, X.Q. Gong, J. Chang, Reusable bioluminescent sensor for ultrasensitive MicroRNA detection based on a target-introducing "Fuel-Loading" mechanism, ACS Appl. Mater. Interfaces 11 (2019) 38586–38594.
[26] S. Liu, Y. Wang, J. Ming, Y. Lin, C. Cheng, F. Li, Enzyme-free and ultrasensitive electrochemical detection of nucleic acids by target catalyzed hairpin assembly followed with hybridization chain reaction, Biosens. Bioelectron. 49 (2013) 472–477.
[27] S.H. Qian, H.W. Lin, Colorimetric sensor array for detection and identification of organophosphorus and carbamate pesticides, Anal. Chem. 87 (2015) 5395–5400.
[28] W. Li, W. Hao, H. Lou, Y. Fu, Q. Fei, G. He, Enhanced thermal management with microencapsulated phase change material particles infiltrated in cellular metal foam, Energy 127 (2017) 671–679.
[29] T. Shurong, T. Ping, W. Meili, C. Jinghua, L. Guangwen, Z. Lan, A novel colorimetric sensor for Hg(2+) based on hybridization chain reaction and silver nanowire amplification, Chem. Commun. 51 (2015) 15043–15046.
[30] M. Wang, G. Meng, Q. Huang, Iodeosin-based fluorescent and colorimetric sensing for Ag^{+}, Hg^{2+}, Fe^{3+}, and further for halide ions in aqueous solution, RSC Adv. 4 (2014) 8055–8058.
[31] X. Xing, H. Yang, M. Tao, W. Zhang, An overwhelmingly selective colorimetric sensor for Ag^{+} using a simple modified polyacrylonitrile fiber, J. Hazard. Mater. 297 (2015) 207–216.
[32] Y.F. Zhu, Y.S. Wang, B. Zhou, Y.Q. Huang, X.J. Li, S.H. Chen, X.F. Wang, X. Tang, Ultrasensitive detection of Ag(I) based on the conformational switching of a multifunctional aptamer probe induced by silver(I), Spectrochim. Acta A. 189 (2018) 190–194.
[33] A. Ravikumar, P. Panneerselvam, N. Morad, Metal-polydopamine framework as an effective fluorescent quencher for highly sensitive detection of Hg(II) and Ag(I) ions through exonuclease III activity, ACS Appl. Mater. Interfaces 10 (2018) 20550–20558.
[34] R.M. Dirks, N.A. Pierce, Triggered amplification by hybridization chain reaction, Proc. Natl. Acad. Sci. U. S. A. 101 (2004) 15275–15278.
[35] X.X. Zhou, S.Y. Xue, P. Jing, W.J. Xu, A sensitive impedimetric platform biosensing protein: insoluble precipitates based on the biocatalysis of manganese(III) meso-tetrakis (4-N-methylpyridiniumyl)-porphyrinin in HCR-assisted dsDNA, Biosens. Bioelectron. 86 (2016) 656–663.
[36] Y.T. Nie, M.Y. Yang, Y.L. Ding, Gold nanoparticle enhanced hybridization chain reaction as a method for signal amplification. Application to electrochemical immunodetection of the ovarian cancer biomarker carbohydrate antigen 125, Microchim. Acta 185 (2018).
[37] J. Zhuang, L. Fu, M. Xu, H. Yang, G. Chen, D. Tang, Sensitive electrochemical monitoring of nucleic acids coupling DNA nanostructures with hybridization chain reaction, Anal. Chim. Acta 783 (2013) 17–23.
[38] K.J. Feng, J. Liu, L. Deng, H.J. Yu, M.H. Yang, Amperometric detection of microRNA based on DNA-controlled current of a molybdophosphate redox probe and amplification via hybridization chain reaction, Microchim. Acta 185 (2018).
[39] M. Zhao, S.F. Li, Q.H. Zhou, D.M. Zhou, N. He, Z.Y. Qian, Safety evaluation of microbial pesticide (HaNPV) based on PCR method, Front. Chem. Sci. Eng. 13 (2019) 377–384.
[40] J. Ikbal, G.S. Lim, Z. Gao, The hybridization chain reaction in the development of ultrasensitive nucleic acid assays, TrAC Trends Anal. Chem. 64 (2015) 86–99.
[41] H. Zheng, M. Yan, X.X. Fan, D. Sun, S.Y. Yang, L.J. Yang, J.D. Li, Y.B. Jiang, A heptamethine cyanine-based colorimetric and ratiometric fluorescent chemosensor (I) for the selective detection of Ag^{+} in an aqueous medium, Chem. Commun. 43 (2012).
[42] M.H. Chen, H.X. Li, Z.H. Shi, W.P. Peng, Y. Qin, R. Luo, D.M. Zhou, X.Q. Gong, J. Chang, High fluorescence quenching probe-based reverse fluorescence enhancement LFTS coupling with IS-primer amplification reaction for the rapid and sensitive Parkinson Disease-associated MicroRNA detection, Biosens. Bioelectron. 165 (2020).